Quantum Monte Carlo study of the one-dimensional Hubbard model with random hopping and random potentials

A. W. Sandvik* and D. J. Scalapino
Department of Physics, University of California, Santa Barbara, California 93106

P. Henelius
Department of Physics, Åbo Akademi, Porthansgatan 3-5, 20500 Åbo, Finland
(Received 28 April 1994)

We have studied the effects of random-hopping matrix elements and random potentials on the properties of the one-dimensional Hubbard model. Using a quantum Monte Carlo technique, disorder-averaged static spin- and charge-density susceptibilities have been evaluated for various strengths of the disorder. Results for the spin susceptibility at wave number $q = 2k_F$ indicate that this quantity, which is the fastest diverging susceptibility of the pure system, diverges as $T \to 0$ also when there is randomness in the hopping matrix elements, but not in the presence of random potentials. Both types of disorder cause a divergence of the uniform magnetic susceptibility. However, for random potentials a finite critical strength of the disorder appears to be required. At half-filling the transition from Mott (gapped) to Anderson (gapless) insulating behavior has been studied. A critical disorder strength is needed to destroy the gap, in agreement with Ma's renormalization group calculations.

I. INTRODUCTION

Real condensed matter systems are always to some extent disordered, and in many cases the disorder cannot be neglected when attempting to construct a theoretical Hamiltonian for a given physical system. It is therefore important to know the properties of basic quantum many-body models, such as the Hubbard model, in the presence of disorder. The one-dimensional (1D) Hubbard model constitutes an excellent testing ground for this problem for a number of reasons. Experimentally, there are quasi-1D tetracyanoquinodimethan (TCNQ) compounds which are believed to be properly described by a 1D Hubbard model with randomness in its parameters.[1–3] One-dimensional systems are also attractive from a theoretical point of view. Exact solutions can be obtained in many cases, with the use of, e.g., bosonization techniques[4] and the Bethe ansatz.[5] Furthermore, quantum Monte Carlo techniques can provide essentially exact results for large systems at low temperatures, as the so-called fermion "sign problem" can be avoided in one dimension.[6] The properties of the pure 1D Hubbard model are now well known,[5,7–9] which makes this model particularly appropriate for investigating the relevance of disorder. In addition, one hopes that insights into the physics in one dimension will prove useful in understanding higher dimensions as well.

Recent research into disordered interacting 1D fermion systems has been primarily concerned with understanding the nature of a metal-insulator transition driven by the interactions. Several theoretical studies indicate that disorder always leads to localization when the particle-particle interactions are repulsive,[10–12] as in the noninteracting case.[13] A metal-insulator transition is predicted to occur for strong enough attractive interactions.[10–12]

The uniform paramagnetic susceptibility $\chi_s(q = 0)$ of disordered systems has been the subject of several theoretical studies.[3,14–17] This was motivated by the discovery that a class of quasi-1D TCNQ compounds exhibit a low-temperature divergence in the magnetic susceptibility.[1,2] These systems are believed to be well described by a half-filled Hubbard model with disorder, which in the strong coupling limit is equivalent to a spin-$\frac{1}{2}$ antiferromagnetic Heisenberg model with random coupling constants.[1,3] Various theoretical methods have been used to study the Heisenberg model with random exchange. The results are in qualitative agreement, giving roughly similar forms for the low-temperature behavior of the susceptibility.[3,14–17] In particular, Hirsch's renormalization group scheme gives a divergence of the form[17]

$$\chi_s(0) \sim \frac{1}{T \ln^m(T)} \tag{1}$$

with $m \approx 2$. Quantum Monte Carlo results are consistent with this behavior.[18] On the other hand, experimentally the susceptibility of some TCNQ compounds is very accurately described by the form

$$\chi_s(q = 0) \sim \frac{1}{T^\alpha}, \tag{2}$$

with $\alpha \approx 0.55-0.9$, over a wide range of temperatures.[1–3] The reason for the discrepancy between theory and experiment has not yet been accounted for.

A less studied problem is the effect of disorder on the $q = 2k_F$ spin-density susceptibility $\chi_s(2k_F)$ and charge-density susceptibility $\chi_c(2k_F)$. In the pure system $\chi_s(2k_F)$ is the strongest diverging susceptibility, growing faster than $\chi_c(2k_F)$ on account of a logarithmic correction. The exact asymptotic $T \to 0$ form for 1D fermions with repulsive interactions has been obtained using bosonization techniques[4,7] and is given by

$$\chi_s(2k_F) \sim T^{K_\rho - 1} |\ln(T)|^{1/2}, \tag{3}$$

with a model dependent K_ρ. For the Hubbard model, Schulz recently calculated K_ρ as a function of the doping and the interaction strength using the Bethe ansatz,[7] and the form of the divergence is hence known exactly. Renormalization group techniques in the "g-ology" formalism, as well as the bosonization method, have been used to study the $q = 2k_F$ susceptibilities of 1D interacting electrons in a random potential. In the parameter regime corresponding to the Hubbard model, Suzumura and Fukuyama[11] predict that with a strong enough on-site interaction strength U, the system exhibits antiferromagnetic behavior [i.e., power law decaying spin correlation functions and diverging $\chi_s(2k_F)$] even in the disordered case. Their calculation is valid only at weak coupling and in the limit of vanishing disorder however. Giamarchi and Schulz,[12] taking into account the effects of finite disorder, found that the renormalization equations scale to a strongly disordered regime, where they are no longer valid. The disordered system is predicted to be similar to a random antiferromagnet, with localized spins. The antiferromagnetic Heisenberg model with random exchange is of some relevance in understanding this problem. Quantum Monte Carlo results indicate that the staggered susceptibility of this model diverges, but slower than for the pure system.[18] For the Hubbard model, quantum Monte Carlo results show a suppression of $\chi_s(2k_F)$,[19,20] but no numerical results for the temperature dependence have been reported so far.

Numerical evaluations of disorder-averaged expectation values require a considerable computational effort, as one has to carry out calculations for a large number of realizations of the disorder in order to obtain meaningful results. In Ref. 20 an alternative method for studying the sensitivity to randomness was suggested and applied to the 1D Hubbard model. For finite disorder, the brute force averaging method is the only reliable method however. Using this approach, we have studied the 1D Hubbard model with random-hopping matrix elements and random potentials. The computations were carried out on a parallel computer,[21] which allowed us to run 96 disorder realizations simultaneously. Here results for the temperature dependence of $\chi_s(2k_F)$ and $\chi_s(q \to 0)$ are presented both for half-filled and doped systems. In addition, at half-filling the charge response $\chi_c(q \to 0)$ is studied in order to obtain information on the effect of the disorder on the Mott-Hubbard gap.

In Sec. II, the model Hamiltonian is introduced and the quantum Monte Carlo technique used is briefly described. In Sec. III, the results are presented. The main results are summarized and discussed in Sec. IV.

II. MODEL AND METHOD

The model Hamiltonian we have studied is the standard 1D repulsive Hubbard Hamiltonian with an impurity term added to it. In standard notation

$$H = -t \sum_{i=1}^{N} \sum_{\sigma=\uparrow,\downarrow} (c^\dagger_{i,\sigma} c_{i+1,\sigma} + c^\dagger_{i+1,\sigma} c_{i,\sigma}) + U \sum_i n_{i,\uparrow} n_{i,\downarrow} + \hat{H}_\alpha, \tag{4}$$

where $\hat{H}_\alpha$ is the term containing the disorder, with $\alpha = t$ for random hopping

$$\hat{H}_t = -\epsilon_t \sum_{i=1}^{N} \sum_{\sigma=\uparrow,\downarrow} \delta_i^t (c^+_{i,\sigma} c_{i+1,\sigma} + c^+_{i+1,\sigma} c_{i,\sigma}) \tag{5}$$

and $\alpha = p$ for random potentials

$$\hat{H}_p = \epsilon_p \sum_{i=1}^{N} \delta_i^p (n_{i\uparrow} + n_{i\downarrow}). \tag{6}$$

The disorder strength is controlled by ϵ_α and the random variables $\{\delta_i^\alpha\}$ are drawn from normalized symmetric distributions ρ_α. Here we take for ρ_α a constant distribution in the interval $[-1, 1]$.

Physical observables of finite disordered systems depend strongly on the particular realization of the disorder. In order to obtain meaningful results, one must therefore average operator expectation values over the disorder realizations. The averaged expectation value of an operator $\hat{A}$ is

$$\langle\langle \hat{A} \rangle\rangle = \int_{-\infty}^{\infty} \prod_{i=1}^{N} d\delta_i^\alpha \rho_\alpha(\delta_i^\alpha) \langle \hat{A} \rangle_{\bar{\delta}}, \tag{7}$$

where $\langle \hat{A} \rangle_{\bar{\delta}}$ is the expectation value of $\hat{A}$ for a given realization $\bar{\delta}$ of the disorder,

$$\langle \hat{A} \rangle_{\bar{\delta}} = \frac{1}{Z_{\bar{\delta}}} \mathrm{Tr}\{\hat{A} e^{-\beta \hat{H}(\bar{\delta})}\}, \qquad Z_{\bar{\delta}} = \mathrm{Tr}\{e^{-\beta \hat{H}(\bar{\delta})}\}. \tag{8}$$

A disorder average $\langle\langle \hat{A} \rangle\rangle$ can be estimated by averaging $\langle \hat{A} \rangle_{\bar{\delta}}$ for a number of randomly selected realizations of the disorder. The desired accuracy of the final result determines the number of realizations needed, which especially for 1D systems can be very large. This type of calculation is ideal for carrying out on a parallel computer, with each processor running its own simulation of a randomly generated disorder realization.

For the calculation of individual expectation values $\langle \hat{A} \rangle_{\bar{\delta}}$ we have used a generalization[22–24] of Handscomb's[25] quantum Monte Carlo technique. With this method the "Trotter error" of standard techniques[6] is avoided. The application of the technique to the 1D Hubbard model is described in Ref. 23. A complete technical account of the method, including recent improvements, and its application to various models will be pre-

sented elsewhere.[24] A brief outline of the technique is included here for completeness.

Consider the Hamiltonian (4) written as

$$\hat{H}(\bar{\delta}) = \sum_{a=1}^{4}\sum_{b=1}^{N}\hat{H}_{a,b}, \tag{9}$$

where

$$\begin{aligned}
\hat{H}_{1,b} &= -(t+\epsilon_t\delta_b^t)(c_{b,\uparrow}^\dagger c_{b+1,\uparrow} + c_{b+1,\uparrow}^\dagger c_{b,\uparrow}),\\
\hat{H}_{2,b} &= -(t+\epsilon_t\delta_b^t)(c_{b,\downarrow}^\dagger c_{b+1,\downarrow} + c_{b+1,\downarrow}^\dagger c_{b,\downarrow}),\\
\hat{H}_{3,b} &= U(n_{b,\uparrow}n_{b,\downarrow}-1) + \epsilon_d(\delta_b^d+\delta_{\max})(n_{b,\uparrow}+n_{b,\downarrow}-2),\\
\hat{H}_{4,b} &= -(t+\epsilon_t\delta_b^t)\ .
\end{aligned} \tag{10}$$

The constant $\delta_{\max}$ in the definition of $\hat{H}_{3,b}$ is the maximum value for the disorder variables δ_i^d. The operators $\hat{H}_{4,i}$ are constant operators added to the Hamiltonian for purposes of the Monte Carlo updating scheme. The Hamiltonians (4) and (9) differ by a constant which plays no role in the simulation.

The starting point of the Monte Carlo method is to Taylor expand $e^{-\hat{H}(\delta)}$ and to write the traces in (8) as sums over diagonal matrix elements of strings of the operators $\hat{H}_{a,b}$. One then obtains an expression suitable for importance sampling,

$$\langle\hat{A}\rangle_{\bar{\delta}} = \frac{\sum_\alpha\sum_n\sum_{S_n}A(\alpha,S_n)W(\alpha,S_n)}{\sum_\alpha\sum_n\sum_{S_n}W(\alpha,S_n)}. \tag{11}$$

Here $W(\alpha,S_n)$ is the weight of the "configuration" (α,S_n) specified by a direct-space state

$$|\alpha\rangle = |n_{1,\uparrow},\ldots,n_{N,\uparrow}\rangle\otimes|n_{1,\downarrow},\ldots,n_{N,\downarrow}\rangle \tag{12}$$

and an index sequence

$$S_n = \binom{a_1}{b_1}_1\binom{a_2}{b_2}_2\cdots\binom{a_n}{b_n}_n, \tag{13}$$

which refers to a string of operators $\prod_{i=1}^n\hat{H}_{a_i,b_i}$. The weight is given by

$$W(\alpha,S_n) = \frac{(-\beta)^n}{n!}\left\langle\alpha\middle|\prod_{i=1}^{n}\hat{H}_{a_i,b_i}\middle|\alpha\right\rangle, \tag{14}$$

which is positive definite with the definition of $H_{3,b}$ in (10) (this is true for open boundary conditions and, for example, for antiperiodic boundary conditions when the number of sites and spin-↑ and spin-↓ particles are all even). The summation in (11) is over all powers n. For a finite system at finite temperature, only n within a well defined regime contribute significantly to the expectation value. The Monte Carlo sampling can be carried out in a space with n unbounded,[23,25] but cutting the summation at some maximum $n=L$ allows for the construction of a faster updating scheme. An L large enough to make the truncation error negligible can be chosen in a self-regulatory fashion[20] and the restriction $n\le L$ is then no approximation in practice (the value of L needed is roughly proportional to the system size and the inverse temperature). Defining an operator $\hat{H}_{0,0}=I$, the unit operator, one can construct a configuration space with index sequences S_L of a fixed length L, by allowing $\binom{a_i}{b_i}=\binom{0}{0}$. The weight then becomes

$$W(\alpha,S_L) = \frac{(-\beta)^n(L-n)!}{L!}\left\langle\alpha\middle|\prod_{i=1}^{L}\hat{H}_{a_i,b_i}\middle|\alpha\right\rangle, \tag{15}$$

where n now denotes the number of non-$\binom{0}{0}$ elements in S_L.

The form of the measuring function $A(\alpha,S_L)$ depends on the type of operator $\hat{A}$ under consideration and is most conveniently defined in terms of the index sequence S_n obtained by omitting the $\binom{0}{0}$ elements in S_L. For an operator $\hat{A}$ which is diagonal in the real-space occupation number basis, the corresponding measuring function can be written as

$$A(\alpha,S_n) = \frac{1}{n+1}\sum_{p=0}^{n}\langle\alpha(p)|\hat{A}|\alpha(p)\rangle, \tag{16}$$

where $|\alpha(p)\rangle$ is the state obtained by operating on $|\alpha\rangle = |\alpha(0)\rangle$ with the first p non-$\binom{0}{0}$ operators of the string,

$$|\alpha(p)\rangle = r\prod_{i=1}^{p}\hat{H}_{a_i,b_i}|\alpha\rangle \tag{17}$$

(r is a normalization factor). Here our main interest is the q-dependent spin- and charge-density susceptibilities

$$\begin{aligned}
\chi_{s,c}(q) = \frac{1}{N}\sum_{j,k}e^{-iq(r_j-r_k)}&\\
\times\int_0^\beta d\tau\langle[n_{j,\uparrow}(\tau)\pm n_{j,\downarrow}(\tau)]&\\
\times[n_{k,\uparrow}(0)\pm n_{k,\downarrow}(0)]&\\
-\langle n_{j,\uparrow}\pm n_{j,\downarrow}\rangle\langle n_{k,\uparrow}\pm n_{k,\downarrow}\rangle\rangle&
\end{aligned} \tag{18}$$

($n_\uparrow - n_\downarrow$=spin, $n_\uparrow + n_\downarrow$=charge). One can show that for any diagonal operators $\hat{A}$ and $\hat{B}$, the measuring function $\chi_{AB}(\alpha,S_n)$ corresponding to the response function operator

$$\hat{\chi}_{AB} = \int_0^\beta d\tau A(\tau)B(0) \tag{19}$$

is given by[22]

$$\begin{aligned}
\chi_{AB}(\alpha,S_n) = \frac{\beta}{n(n+1)}\Bigg[&\left(\sum_{p=0}^{n-1}\langle\alpha(p)|\hat{A}|\alpha(p)\rangle\right)\\
&\times\left(\sum_{p=0}^{n-1}\langle\alpha(p)|\hat{B}|\alpha(p)\rangle\right)\\
&+\sum_{p=0}^{n-1}\langle\alpha(p)|\hat{A}|\alpha(p)\rangle\langle\alpha(p)|\hat{B}|\alpha(p)\rangle\Bigg].
\end{aligned} \tag{20}$$

Hence, with this simulation scheme the integration over imaginary time does not have to be carried out numerically, which is the case with standard quantum Monte Carlo methods.[6]

In a Monte Carlo procedure one starts from some configuration $(\alpha, S_L)_0$ with nonzero weight (15) and proceeds by making a series of changes in $|\alpha\rangle$ and S_L in order to generate a series of configurations $(\alpha, S_L)_1, (\alpha, S_L)_2, \ldots$ A configuration $(\alpha, S_L)_{n+1}$ generated from $(\alpha, S_L)_n$ is accepted or rejected in a standard manner (heat-bath or Metropolis algorithm) based upon the weight ratio $W(\alpha, S_L)_{n+1}/W(\alpha, S_L)_n$. The simulation is started with $|\alpha\rangle$ randomly generated and with an index sequence S_L containing only $\binom{0}{0}$ elements. The updating scheme is constructed such that no attempts to generate zero-weight configurations are made. The following types of "moves" involving the index sequence are performed:

$$\binom{0}{0}_i \leftrightarrow \binom{4}{b}_i , \tag{21a}$$

$$\binom{4}{b}_i \leftrightarrow \binom{3}{c}_i , \tag{21b}$$

$$\binom{1}{b}_i \binom{1}{b}_j \leftrightarrow \binom{4}{b}_i \binom{4}{b}_j , \tag{21c}$$

$$\binom{2}{b}_i \binom{2}{b}_j \leftrightarrow \binom{4}{b}_i \binom{4}{b}_j . \tag{21d}$$

Moves of particles in the state $|\alpha\rangle$ can also be carried out, but are actually not needed in the canonical ensemble, since all states with a given number of spin $\uparrow$ and spin $\downarrow$ can be generated by the moves (21a)–(21d). With the moves in (21) one can generate all contributing index sequences for an open chain. With periodic boundary conditions additional, more complicated moves are needed to sample configurations with a nonzero "winding number."[6] These moves are important only for small systems, as they are associated with the boundary conditions. Details of the updating scheme are given in Refs. 23 and 24. During the equilibration part of the simulation, the length of the index sequence is increased as long as n [the number of non-$\binom{0}{0}$ elements] is growing and is always kept larger than the maximum n reached. In this way, the restriction $n \leq L$ does not in practice affect the accuracy of the results.

A Monte Carlo step is defined as a series of the moves (21a) and (21b) attempted at all positions of S_L and a number of moves (21c) and (21d) resulting in approximately 30–50 % of the elements involved being changed. Measurements are carried out with an interval of $10 - 20$ Monte Carlo steps. The number of operations performed in one Monte Carlo step scales linearly with the system size and approximately linearly with the inverse temperature.

The implementation for parallel processing is trivial in this case. We simply run the same Monte Carlo code on 96 "worker" processors, each with its own realization of the disorder. The distribution of the tasks and the subsequent averaging procedure is carried out by a "master" processor.

In a simulation of a pure system, the number of Monte Carlo steps needed to bring the simulation to equilibrium is normally small compared to the total length of the simulation. When estimating a disorder average, one clearly wants to do runs for as many realizations as possible within a given amount of computer time. It is statistically advantageous to do a large number of short runs for different realizations instead of doing a few long accurate calculations. The time needed for equilibration is here of some concern, as this is the minimum time needed for a run. In order to check that equilibrium is reached, it is useful to calculate expectation values as functions of Monte Carlo "time." In Fig. 1 some results of such a calculation for a 32-site system are shown during a run consisting of 5×10^4 equilibration steps followed by 10^5 steps for measurements. The values shown as functions of time represent averages of the results from the 96 computer nodes used simultaneously. The initial rapid changes and subsequent leveling off as equilibrium is reached are clearly visible. The time needed for equilibration increases with the system size. Based on available computer resources we decided to study 32-site systems. This is not quite large enough for observing the exact asymptotic behavior of pure systems. In Fig. 2 results for the $q = 2k_F$ spin susceptibility [given by Eq. (18)]

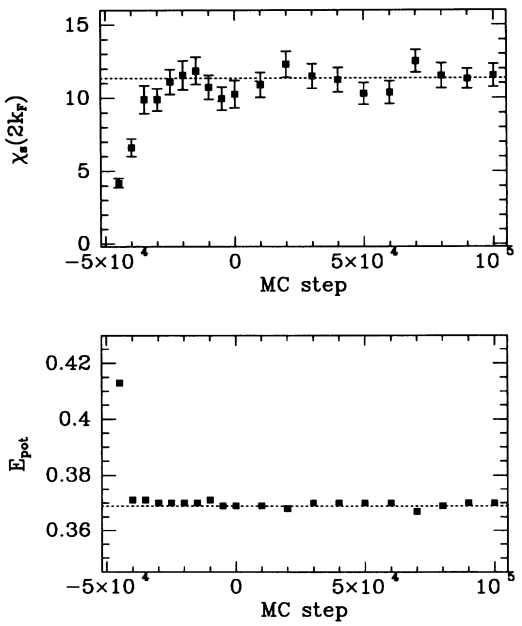

FIG. 1. The $2k_F$ spin susceptibility (top) and the potential energy (bottom) versus Monte Carlo "time" for a half-filled 32-site system with site disorder strength $\epsilon_p = 2$ at $\beta = 12$. Each point represents an average of the results of 96 simultaneous simulations over a number of Monte Carlo steps corresponding to the horizontal distance between the point and the preceding point. The MC steps < 0 are equilibration steps, during which the length of the index sequence may be increased. The dashed lines represent the averages over the "measurement steps" (MC step > 0 in the graphs).

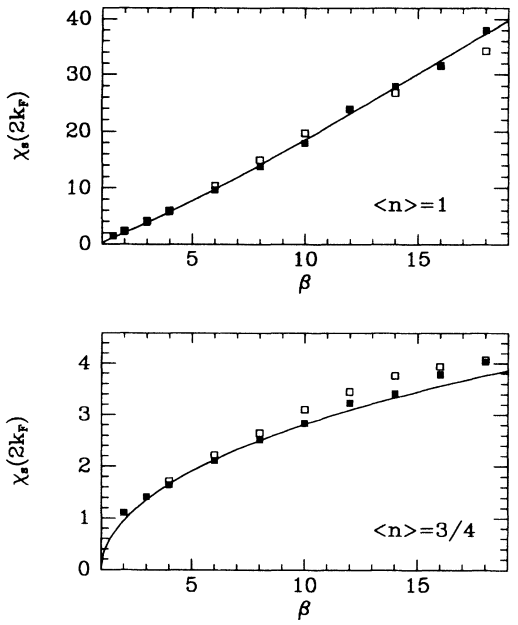

FIG. 2. The spin susceptibility $\chi_s(2k_F)$ versus the inverse temperature for system sizes $N = 32$ (open squares) and $N = 64$ (solid squares) at fillings $\langle n\rangle = 1$ and $\langle n\rangle = 0.75$. Statistical errors are of the order of the size of the symbols. The curves are the known low-temperature forms given by Eq. (3) with $K_\rho = 0$ for $\langle n\rangle = 1$ and $K_\rho = 0.70$ for $\langle n\rangle = \frac{3}{4}$.

for pure systems with $U = 4t$, $N = 32$, and $N = 64$ are shown versus the inverse temperature $\beta = t/T$, along with the known asymptotic form (3). At half-filling the $N = 64$ points quite accurately follow the asymptotic form, whereas the $N = 32$ data initially rise slightly too fast before leveling off due to the finite size. At a filling $\langle n\rangle = 0.75$ the finite-size effects are even stronger. Again, the increase with β is too rapid before the low-temperature saturation and even $N = 64$ is not large enough to give the correct form over a wide range of temperatures. The finite-size effects are smaller for disordered systems, however, and 32 sites should be large enough for capturing the effects of the disorder. Most results presented here were obtained in simulations consisting of 5×10^4+10^5 Monte Carlo steps on 96 computer nodes. In some cases longer equilibration times were needed and in some cases several runs had to be made in order to obtain accurate enough final results. We believe that most of our results are free from systematical errors due to insufficient equilibration. However, for the strongest disorder strengths studied ($\epsilon_t = 0.9$ and $\epsilon_p = 4$) there are probably slight effects of this nature. Some results obtained with very long equilibration times indicate that this error is comparable to the statistical errors.

At the lowest temperatures studied, more than 30 h of computer time were needed for each set of $N = 32$ runs. For this type of simulation, the total computing power of the 96 nodes used corresponds to approximately 10 DECstation 5000 workstations.

III. RESULTS

In this section results for the Hubbard Hamiltonian (4) with random-hopping matrix elements and random potentials are presented for both half-filled and doped systems. Simulations were carried out for several strengths of the disorder, with the on-site Coulomb interaction U kept equal to the bandwidth $4t$. The disorder variables $\epsilon_\alpha \delta_i^\alpha$ in (5) and (6) were chosen uniformly distributed in an interval $[-\epsilon_\alpha, \epsilon_\alpha]$. For random hopping, disorder strengths ϵ_t =0.3, 0.6, and 0.9 were studied, and for random potentials ϵ_p=1, 2, and 4 (all in units of t). For pure systems, all results shown are for $N = 64$, whereas the results for disordered systems are for $N = 32$.

Below, the $q = 2k_F$ spin susceptibilities are compared to the asymptotic form (3) for the pure Hubbard model, in order to determine whether this form still is relevant, with a K_ρ which may be renormalized by the disorder. The uniform magnetic susceptibility $\chi_s(q \to 0)$ is also studied. In the half-filled case another interesting aspect is the effect of disorder on the charge gap. The results in Ref. 20 for the effect of weak disorder on the charge susceptibility $\chi_c(q)$ in the limit $q \to 0$ indicate that a finite amount of disorder is needed to destroy the gap, in agreement with renormalization group calculations.[26] Here χ_c in the presence of finite disorder gives information on the transition from Mott (finite gap) to Anderson (gapless) insulating behavior.

A. Half-filled systems

We first discuss the half-filled case ($\langle n\rangle = 1$). In Fig. 3 the spin susceptibility $\chi_s(q)$ [Eq. (18)] is shown versus the wave number q for systems with different strengths of hopping disorder at a low temperature ($\beta = 16$). As expected, the antiferromagnetic peak is strongly suppressed and the long-wavelength susceptibility is enhanced, the effect increasing with increasing disorder strength. In Fig. 4 the temperature dependence of $\chi_s(q = 2k_F = \pi)$ is compared to the asymptotic form for the pure system Eq. (3). If this form applies, $\chi_s(2k_F)/|\ln(\beta)|^{1/2}$ graphed versus $\ln(\beta)$ should produce points falling onto straight lines with slopes $1 - K_\rho$. This seems indeed to be the case for all hopping-disorder strengths studied here, with an exponent K_ρ which depends on the disorder strength. In the pure system $K_\rho = 0$ at half-filling, as for the 1D spin-$\frac{1}{2}$ Heisenberg chain.[4] Least-squares fits of straight lines to the low-temperature points in Fig. 4 gives the exponents $K_\rho = 0.00 \pm 0.02$, 0.22 ± 0.02, 0.39 ± 0.04, and 0.50 ± 0.04 for $\epsilon_t = 0$, 0.3, 0.6, and 0.9, respectively. The highest temperature at which the asymptotic form fits the data decreases with increasing disorder, probably reflecting an energy scale associated with the weakest hopping matrix elements of the disordered systems, $t_{\min} = t(1 - \epsilon_t)$. One cannot completely rule out the possibility that the behavior observed in the temperature regime studied here is only relevant down to a low temperature at which $\chi_s(\pi)$ saturates. The energy scale of such a crossover must be very low, however, as there are no indications of satura-

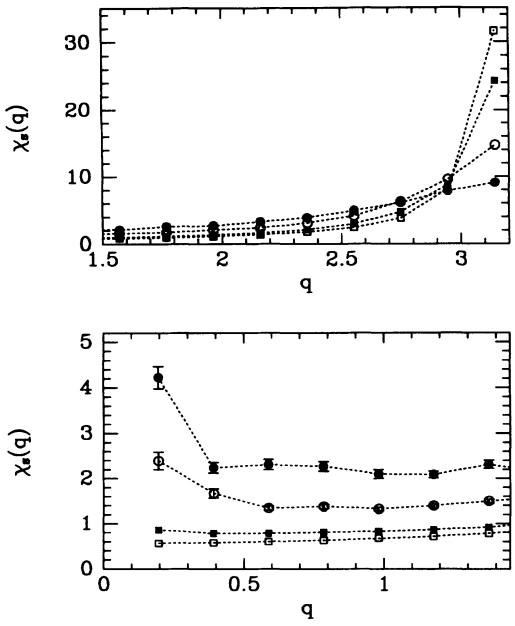

FIG. 3. The spin susceptibility at half-filling in the short- (top) and long- (bottom) wavelength regimes for hopping disorder strengths $\epsilon_t = 0$ (open squares), 0.3 (solid squares), 0.6 (open circles), and 0.9 (solid circles). The inverse temperature is $\beta = 16$.

tion for $\beta \leq 18$ for any of the disorder strengths studied here.

Since the systems studied have fixed numbers of spin-↑ and spin-↓ electrons, the uniform magnetic susceptibility $\chi_s(q = 0)$ vanishes identically. Results are therefore shown for the lowest nonzero value of q, i.e., $q_1 = 2\pi/N$. The susceptibility at $q = q_1$ will approach the uniform susceptibility if the system is large enough since $\chi_s(q_1)$ roughly corresponds to the uniform susceptibility of a system of size $N/2$. In Fig. 5 $\ln[\chi_S(q_1)]$ is graphed versus $\ln(\beta)$. For all disorder strengths a linear behavior is seen at low temperatures, indicating a temperature dependence of the form (2), i.e., the form observed experimentally in some TCNQ compounds. Values for α reported for these systems are in the range $0.55 - 0.9$.[1–3] Here least-squares fits give $\alpha = 0.29 \pm 0.07$, 0.72 ± 0.04, and 0.89 ± 0.04 for $\epsilon_t = 0.3$, 0.6, and 0.9, respectively. The results are not well described by the form (1) with $m \approx 2$.

Results for the q-dependent spin susceptibility in the presence of random potentials are shown in Fig. 6. The behavior in this case is markedly different from the random-hopping case. For the weaker disorder strengths, virtually no effects are seen at long wavelengths, while the response at $q = \pi$ is suppressed as before. In addition, $\chi_s(q)$ is also suppressed over a wide regime around the peak, where Fig. 3 shows an enhancement in the random hopping case. In Fig. 7 the temperature dependence of $\chi_s(\pi)$ is analyzed. For $\epsilon_p = 1$, the behavior is as in the pure system up to approximately $\beta = 10$, where the increase becomes slower. As shown in Fig. 1, at this temperature finite-size effects are visible in pure 32-site systems. However, in that case the $N = 32$ susceptibility actually grows faster than the asymptotic form, whereas here there is a clear suppression for $\beta > 10$. The suppression is therefore caused by the disorder and not by the finite size. For $\epsilon_p = 2$, the asymptotic form (3) also seems to apply in a fairly wide temperature regime, but at low temperatures the slope decreases. For $\epsilon_p = 4$, the response is very strongly suppressed. There is a narrow regime where $\ln[\chi_s(\pi)]/\ln(\beta)^{1/2}$ increases slightly. There is then a leveling off and the low-temperature behavior is consistent with $K_\rho = 1$, which would correspond to a logarithmic divergence of $\chi_s(\pi)$. Clearly, larger systems at lower temperatures have to be studied in order to determine the low-temperature behavior more accu-

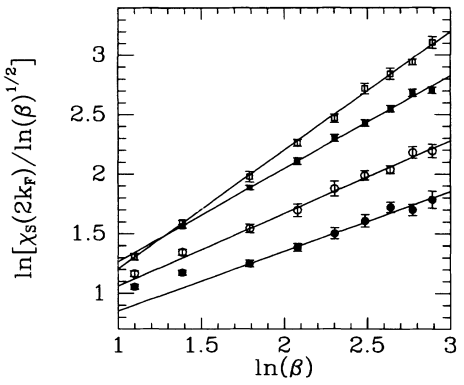

FIG. 4. The $q = 2k_F = \pi$ spin susceptibility for half-filled systems with hopping disorder, graphed so that the points should follow straight lines if the asymptotic form $\chi_s \sim T^{K_\rho - 1}|\ln(T)|^{1/2}$ is obeyed. The disorder strengths are $\epsilon_t = 0$ (open squares), 0.3 (solid squares), 0.6 (open circles), and 0.9 (solid circles). The solid lines are least-squares fits, giving $K_\rho = 0.00 \pm 0.02$ ($\epsilon_t = 0$), 0.22 ± 0.02 ($\epsilon_t = 0.3$), 0.39 ± 0.04 ($\epsilon_t = 0.6$), and 0.50 ± 0.04 ($\epsilon_t = 0.9$).

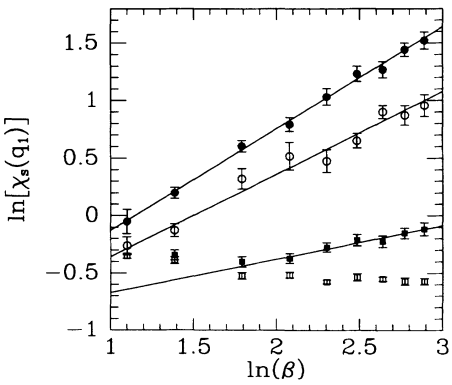

FIG. 5. The logarithm of the long-wavelength spin susceptibility ($q_1 = 2\pi/N$) versus the logarithm of the inverse temperature for half-filled systems with hopping disorder strengths $\epsilon_t = 0$ (open squares), 0.3 (solid squares), 0.6 (open circles), and 0.9 (solid circles). The straight lines are least-squares fits, with slopes $\alpha = 0.29 \pm 0.07$ ($\epsilon_t = 0.3$), 0.72 ± 0.04 ($\epsilon_t = 0.6$), and 0.89 ± 0.04 ($\epsilon_t = 0.9$).

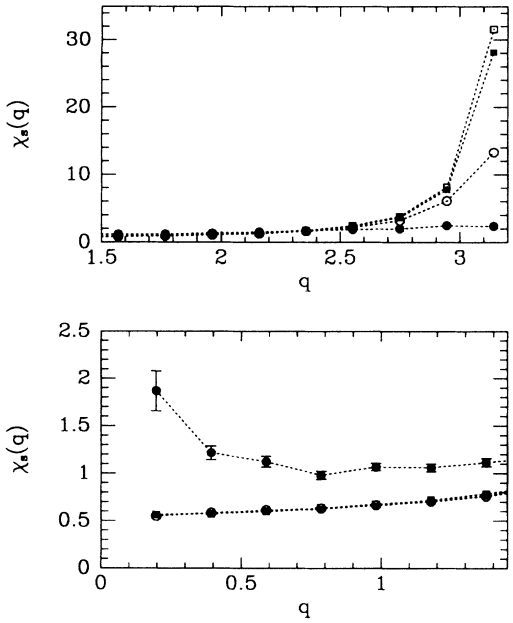

FIG. 6. The spin susceptibility at half-filling in the short- (top) and long- (bottom) wavelength regimes for random potential strengths $\epsilon_p = 0$ (open squares), 1.0 (solid squares), 2.0 (open circles), and 4.0 (solid circles). The inverse temperature is $\beta = 16$. In the bottom graph, the results for $\epsilon_p = 0$, 1, and 2 are indistinguishable within statistical errors.

rately. The results shown in Fig. 7 do, however, indicate that the pure-system asymptotic form does not apply at low temperatures, suggesting that $\chi_s(\pi)$ might saturate as $T \to 0$.

The $q \to 0$ spin susceptibility is analyzed in Fig. 8. Here a divergence is seen only for $\epsilon_p = 4$. For the weaker disorder strengths the results are indistinguishable from the pure system susceptibility. In Ref. 20 we reported

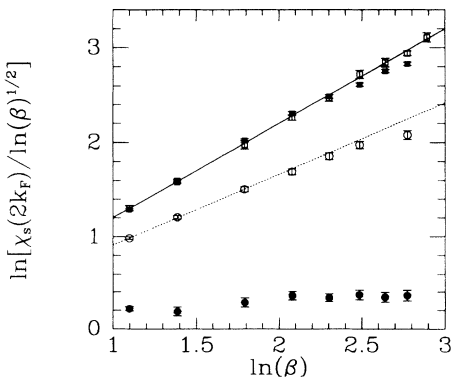

FIG. 7. The $q = 2k_F$ spin susceptibility for half-filled systems with random potentials, graphed as in Fig. 4. The disorder strengths are $\epsilon_p = 0$ (open squares), 1.0 (solid squares), 2.0 (open circles), and 4.0 (solid circles). The solid line is a least-squares fit to the pure-system results, giving $K_\rho = 0.00 \pm 0.02$. The dashed line is a fit to $\epsilon_p = 2$ results for $\beta \leq 6$ and corresponds to $K_\rho = 0.25$.

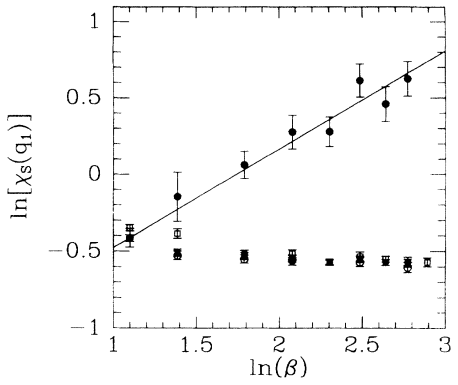

FIG. 8. The logarithm of the long-wavelength spin susceptibility ($q_1 = 2\pi/N$) versus the logarithm of the inverse temperature for half-filled systems with random potential strengths $\epsilon_p = 0$ (open squares), 1.0 (solid squares), 2.0 (open circles), and 4.0 (solid circles). The straight line is a least-squares fit to the $\epsilon_p = 4.0$ points and has slope $\alpha = 0.64 \pm 0.06$.

calculations of the lowest-order effects of disorder on the q-dependent susceptibility in terms of the second derivative with respect to the disorder strength

$$D_\alpha[\chi_s(q)] = \frac{\left.\frac{\partial^2 \chi_s(q)}{\partial \epsilon_\alpha^2}\right|_{\epsilon_\alpha=0}}{\int d\delta \rho_\alpha(\delta)\delta^2} \tag{22}$$

(the first derivative vanishes). As defined above, D_α is independent of the distribution ρ_α and is thus a property of the pure system which can be calculated in a single Monte Carlo simulation, without disorder averaging. In Fig. 9 $D_t[\chi_s]$ and $D_p[\chi_s]$ are shown versus the wave number for a $N = 64$ system at $\beta = 24$. The hopping disorder derivative $D_t[\chi_s(q)]$ in the limit $q \to 0$ is large and positive, indicating that any finite amount of hopping disorder leads to an enhancement of $\chi_s(q \to 0)$ and presumably a divergence as $T \to 0$ ($D_t[\chi(q \to 0)]$ grows rapidly as the temperature is lowered[20]). In contrast, the random potential derivative $D_t[\chi_s(q \to 0)]$ is zero within

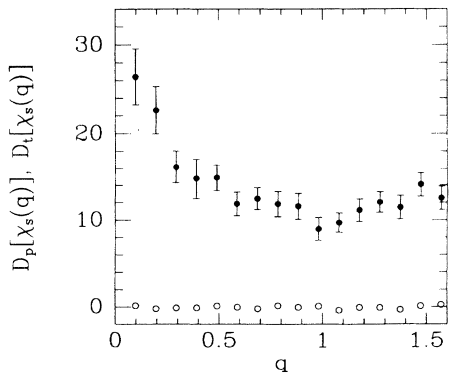

FIG. 9. The disorder derivatives $D_t[\chi_s(q)]$ (solid circles) and $D_p[\chi_s(q)]$ (open circles) for a half-filled $N = 64$ system at inverse temperature $\beta = 24$.

statistical errors. If the disorder is weak the enhancement of $\chi_s(q \to 0)$ may occur only at very low temperatures. However, in view of the fact that no effects are seen for a potential disorder as strong as $\epsilon_p = 2$ at $\beta = 16$ (Fig. 6) and that the corresponding disorder derivative vanishes, we conjecture that a finite critical strength of this type of disorder is needed to cause a divergence.

To further investigate the differences in the effects of the two types of disorder on the uniform magnetic susceptibility, we carried out exact diagonalizations for small systems ($N = 4$ and 6). In order to be able to observe the effect on $\chi_s(0)$ directly, we studied ensembles with $n = n_\uparrow + n_\downarrow$ fixed, but $n_\uparrow$ and $n_\downarrow$ allowed to fluctuate. Averages over 200–500 realizations of random hopping and random potentials were calculated. Due to the large gap between the ground state and the excited states in the small systems studied, the uniform susceptibility of the pure system vanishes rapidly as the temperature is lowered below $T = 0.5t$. Nevertheless, the results give some additional insights into the effect of the disorder. In Fig. 10 results for random hopping are compared to pure-system results. For $T < 0.5$, the susceptibility is enhanced for all disorder strengths studied. The enhancement is stronger for $N = 6$ than for $N = 4$. In Fig. 11 results for random potentials are shown. Here the susceptibility of weakly disordered systems is actually suppressed at all temperatures. The high-temperature susceptibility decreases as the disorder strength is increased, reflecting a lowered local magnetic moment due to an increased density of doubly occupied sites. At a size-dependent disorder strength the low-temperature susceptibility starts to increase with the disorder. These results are consistent with the quantum Monte Carlo results for $N = 32$, where an enhancement of $\chi_s(q \to 0)$ was noted for $\epsilon_p = 4$, but not for $\epsilon_p = 2$ (Figs. 6 and 8). It seems likely that a critical potential disorder strength indeed is required for the susceptibility of an infinite system to diverge.

The behavior of the charge-density susceptibility $\chi_c(q)$ in the $q \to 0$ limit (the compressibility) signals the presence or absence of a charge gap. Figure 12 shows the q-dependent low-temperature charge susceptibility for hopping disordered systems. In the pure system, and for $\epsilon_t = 0.3$, the susceptibility vanishes as $q \to 0$, indicating that there is a charge gap also in a weakly hopping

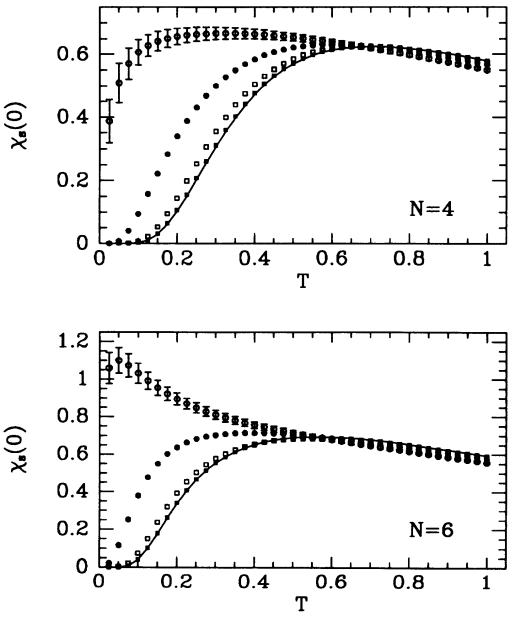

FIG. 10. Exact diagonalization results for the uniform spin susceptibility versus the temperature for $N = 4$ and 6 systems with random hopping. The solid lines are for pure systems. Solid squares are for $\epsilon_t = 0.1$, open squares for $\epsilon_t = 0.3$, solid circles for $\epsilon_t = 0.6$, and open circles for $\epsilon_t = 0.9$.

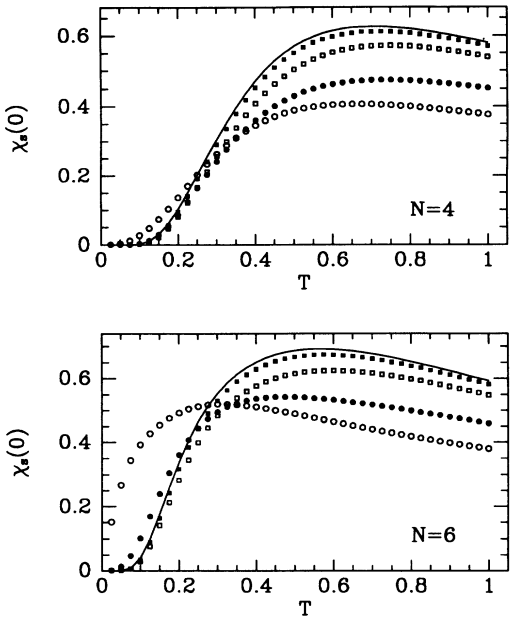

FIG. 11. Exact diagonalization results for the uniform spin susceptibility versus the temperature for $N = 4$ and 6 systems with random potentials. The solid lines are for pure systems. Solid squares are for $\epsilon_p = 1$, open squares for $\epsilon_p = 2$, solid circles for $\epsilon_p = 4$, and open circles for $\epsilon_p = 6$.

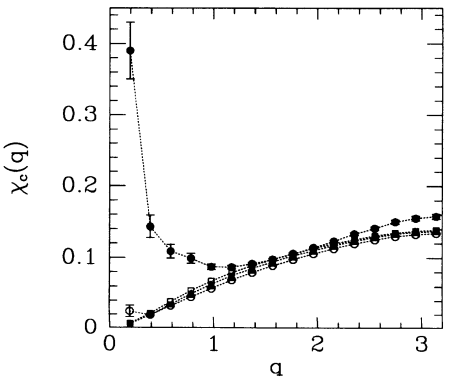

FIG. 12. The charge-density susceptibility versus the wave number for half-filled systems with hopping disorder strengths $\epsilon_t = 0$ (open squares), 0.3 (solid squares), 0.6 (open circles), and 0.9 (solid circles). The inverse temperature is $\beta = 16$.

disordered system. For $\epsilon_t = 0.9$ the $q \to 0$ response is enhanced, indicating that the disorder is strong enough to destroy the gap. For $\epsilon_t = 0.6$ the response also seems to be slightly enhanced at $q = q_1 = 2\pi/N$, but the statistical error is rather large. The critical strength at $U = 4t$ is probably quite close to $\epsilon_t = 0.6$. The charge response in the presence of random potentials is graphed in Fig. 13. Again, for the weakest disorder strength studied ($\epsilon_p = 1$) the gap is still present. The $q \to 0$ behavior for $\epsilon_p = 2$ is different, extrapolating to a finite value at $q = 0$. Thus the Mott-Anderson transition for $U = 4t$ occurs for ϵ_p between 1 and 2. With random potentials the response is strongly enhanced for all q as the disorder strength is increased above the critical strength, in contrast to the random-hopping case where there is a strong effect only at long wavelengths.

For a Gaussian distribution of random potentials, Ma's renormalization group result[26] for the critical width W of the distribution at $U = 4t$ is $W \approx 0.7$. It would clearly be interesting to compare the renormalization group phase boundary with Monte Carlo results for this disorder distribution.

B. Doped systems

In this section, we will consider a doped system with a filling $\langle n \rangle = \frac{3}{4}$. The q-dependent spin susceptibility at $\beta = 16$ is graphed for systems with hopping disorder in Fig. 14 and for potential disorder in Fig. 15. As in the half-filled case, hopping disorder suppresses the $q = 2k_F$ peak and enhances the response at other wavelengths. Unlike in the half-filled case, random potentials now slightly enhance the $q \to 0$ response even for $\epsilon_p = 1$. The response at $q = \pi$ is also strongly enhanced. For $\epsilon_p = 4$, $\chi_s(\pi)$ is actually larger than $\chi_s(2k_F)$.

The temperature dependence of $\chi_s(2k_F)$ in the presence of hopping disorder is analyzed in Fig. 16. The data are consistent with a divergence of the pure-system form, with $K_\rho = 0.70 \pm 0.04$ for $\epsilon_t = 0.6$ and $K_\rho = 0.73 \pm 0.04$ for $\epsilon_t = 0.9$. The results shown for a pure system with

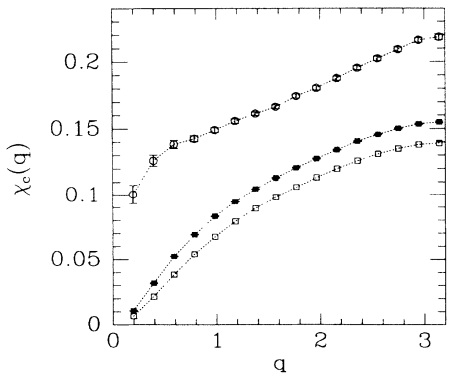

FIG. 13. The charge-density susceptibility versus the wave number for half-filled systems with site disorder strengths $\epsilon_p = 0$ (open squares), 1 (solid squares), and 2 (open circles). The inverse temperature is $\beta = 16$.

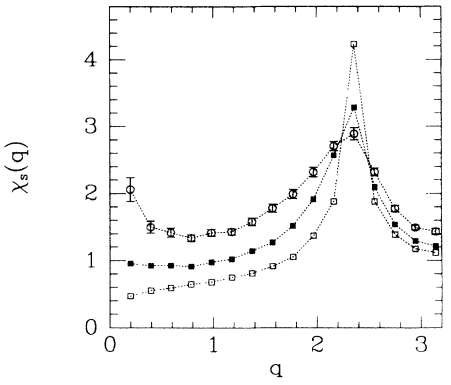

FIG. 14. The q-dependent spin susceptibility at filling $\langle n \rangle = \frac{3}{4}$ for hopping disorder strengths $\epsilon_t = 0$ (open squares), 0.6 (solid squares), and 0.9 (open circles). The inverse temperature is $\beta = 16$.

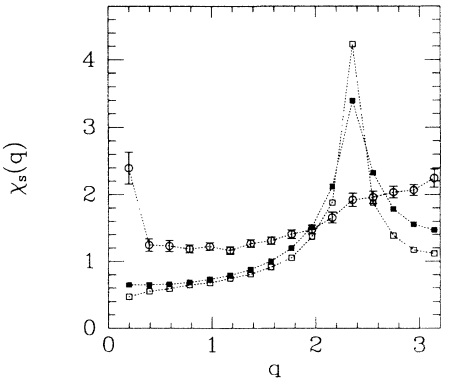

FIG. 15. The q-dependent spin susceptibility at filling $\langle n \rangle = \frac{3}{4}$ for site disorder strengths $\epsilon_p = 0$ (open squares), 1 (solid squares), and 4 (open circles). The inverse temperature is $\beta = 16$.

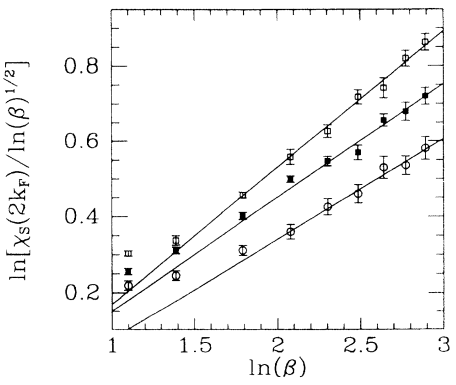

FIG. 16. The $q = 2k_F$ spin susceptibility for $\langle n \rangle = \frac{3}{4}$ in the presence of hopping disorder. This has been plotted so that the points should follow straight lines if the asymptotic form $\chi_s \sim T^{K_\rho - 1} |\ln(T)|^{1/2}$ is obeyed. The disorder strengths are $\epsilon_t = 0$ (open squares), 0.6 (solid squares), and 0.9 (open circles). The solid lines are least-squares fits, giving $K_\rho = 0.65 \pm 0.02$ ($\epsilon_t = 0$), 0.70 ± 0.04 ($\epsilon_t = 0.6$), and 0.73 ± 0.04 ($\epsilon_t = 0.9$).

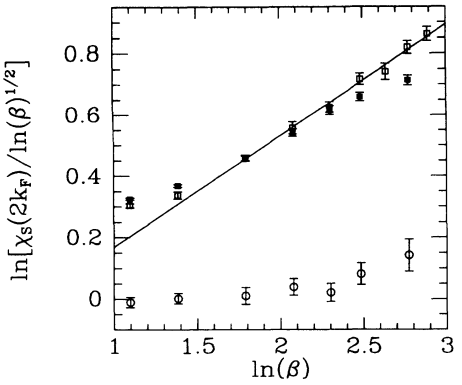

FIG. 17. The $q = 2k_F$ spin susceptibility for $\langle n \rangle = \frac{3}{4}$ in the presence of site disorder graphed as in Fig. 16. The disorder strengths are $\epsilon_p = 0$ (open squares), 1 (solid squares), and 4 (open circles). The solid line is a fit to the pure-system results, with $K_\rho = 0.65 \pm 0.02$.

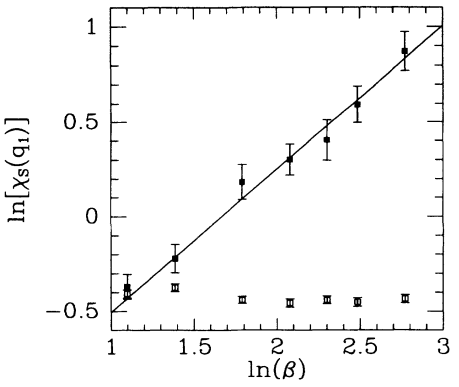

FIG. 19. The logarithm of the long-wavelength spin susceptibility ($q_1 = 2\pi/N$) versus the logarithm of the inverse temperature for systems at filling $\langle n \rangle = \frac{3}{4}$, with site disorder strengths $\epsilon_p = 1$ (open squares) and 4 (solid squares). The straight line has slope $\alpha = 0.75 \pm 0.05$.

$N = 64$ give $K_\rho = 0.65 \pm 0.02$, which is slightly lower than the known[7] value $K_\rho = 0.70$. The results shown in Fig. 1 indicate that this discrepancy is a finite-size effect. The dependence of K_ρ on the hopping disorder strength is thus very weak away from half-filling, and in fact our results are consistent with a K_ρ which is not changed by the disorder in this case.

Results for the temperature dependence of $\chi_s(2k_F)$ in the presence of random potentials are shown in Fig. 17. For $\epsilon_p = 1$ there is an intermediate temperature regime where the pure-system asymptotic form is approximately obeyed. At lower temperatures the growth with β becomes much slower, however, indicating that $\chi_s(2k_F)$ does not diverge in the disordered system. For $\epsilon_p = 4$ the response is very strongly suppressed, but still increases slightly with β in the temperature regime studied.

In Figs. 18 and 19 the long-wavelength spin susceptibility is graphed for hopping- and site-disordered systems, respectively. Again the form (2) seems to describe the $\epsilon_p = 4$ data well at low temperatures. For $\epsilon_p = 1$ the susceptibility does not appear to diverge, although it is slightly enhanced over the pure-system value (Fig. 15). It seems likely that a critical disorder strength is required to cause a divergence, as was suggested above to be the case at half-filling. For hopping disorder, least-squares fits give the exponents $\alpha = 0.27 \pm 0.04$ for $\epsilon_t = 0.6$ and $\alpha = 0.71 \pm 0.04$ for $\epsilon_t = 0.9$. For random potentials of strength $\epsilon_p = 4$ the exponent obtained is $\alpha = 0.75 \pm 0.05$.

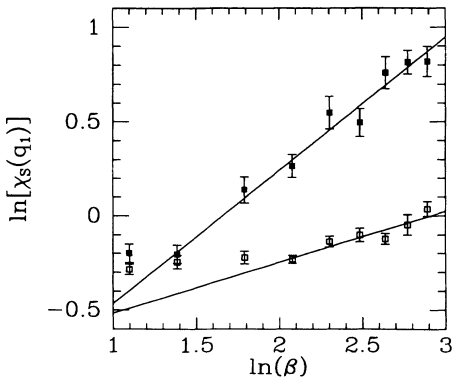

FIG. 18. The logarithm of the long-wavelength spin susceptibility ($q_1 = 2\pi/N$) versus the logarithm of the inverse temperature for systems at filling $\langle n \rangle = \frac{3}{4}$, with hopping disorder strengths $\epsilon_t = 0.6$ (open squares) and 0.9 (solid squares). The straight lines are least-squares fits with slopes $\alpha = 0.27 \pm 0.04$ ($\epsilon_t = 0.6$) and 0.71 ± 0.04 ($\epsilon_t = 0.9$).

IV. SUMMARY AND DISCUSSION

In summary, the 1D Hubbard model with random-hopping matrix elements and random potentials has been studied numerically using the brute-force method of averaging quantum Monte Carlo results for a large number of realizations of the disorder. Results for the static spin- and charge-density susceptibilities in the presence of the two types of disorder have been presented.

Both disorder types lead to a $T \to 0$ divergence of the uniform magnetic susceptibility. However, the results indicate that any finite amount of randomness in the hopping matrix elements causes a divergence, whereas a critical random potential strength appears to be required. In both cases the divergence is consistent with the form $\chi \sim T^{-\alpha}$, which is the form found experimentally in a class of TCNQ compounds.[1–3]

The temperature dependence of the $q = 2k_F$ spin susceptibility was also studied. In a pure system, this susceptibility is the strongest diverging one, having the low-temperature form $\chi_S(2k_F) \sim |\ln(T)|^{1/2} T^{K_\rho - 1}$, with K_ρ dependent on the band filling and U.[7] The results presented here indicate that $\chi_s(2k_F)$ diverges also in the presence of hopping disorder. The low-temperature behavior is consistent with the above form for the divergence. At half-filling K_ρ depends strongly on the disorder, whereas away from half-filling our results show

no statistically significant dependence on the disorder strength. In a pure system with a filling $\langle n \rangle = 1 \pm \delta$, $K_\rho \to \frac{1}{2}$ as $\delta \to 0$, whereas exactly at half-filling ($\delta = 0$) umklapp scattering causes the exponent to change to $K_\rho = 0$, i.e., it is different from the $\delta \to 0$ value. Hence our results for hopping disorder indicate that this kind of disorder mainly affects the umklapp processes, thereby increasing K_ρ significantly at half-filling, but not away from half-filling. For the largest disorder strength studied here, the value of K_ρ is consistent with the pure-system value in the limit $\delta \to 0$ ($K_\rho = 0.5$), indicating that umklapp plays no role. It would clearly be of importance to investigate the behavior for even stronger disorder, to make clear whether $K_\rho = 0.5$ is indeed the limiting value as $\epsilon_t \to 1$.

For random potentials, the results for $\chi_s(2k_F)$ are not consistent with the pure-system form at the lowest temperatures studied and it seems most likely that $\chi_s(2k_F)$ does not diverge in this case. The reasons for the markedly different effects of the two types of disorder deserve further investigations.

In order to obtain information on the presence or absence of a Mott-Hubbard gap at half-filling, the $q \to 0$ limit of the charge-density susceptibility was studied. The results indicate that a finite amount of disorder is needed to cause the transition from the gapped (Mott) to the gapless (Anderson) insulating state, in agreement with Ma's renormalization group results.[26]

ACKNOWLEDGMENTS

We would like to thank L. Caron for discussions and the Department of Computer Science at Åbo Akademi for a generous allocation of time on their Hathi-2 parallel computer. This work was supported in part by the Department of Energy under Grant No. DE-FG03-85ER45197.

* On leave from Department of Physics, Åbo Akademi, Åbo, Finland.

[1] L.N. Bulaevskii *et al.*, Zh. Eksp. Teor. Fiz. **62**, 725 (1972) [Sov. Phys. JETP **35**, 384 (1972)].

[2] L.J. Azvedo and W.G. Clark, Phys. Rev. B **16**, 3252 (1977); J. Sanny, G. Grüner, and W.G. Clark, Solid State Commun. **35**, 657 (1980); H.M. Bozler, C.M. Gould, and W.G. Clark, Phys. Rev. Lett. **45**, 1303 (1980); L.C. Tippie and W.G. Clark, Phys. Rev. B **23**, 5846 (1981).

[3] G. Theodorou and M. Cohen, Phys. Rev. Lett. **37**, 1014 (1976); G. Theodorou, Phys. Rev. B **16**, 2254 (1977); **16**, 2273 (1977).

[4] T. Giamarchi and H.J. Schulz, Phys. Rev. B **39**, 4620 (1989); I. Affleck *et al.*, J. Phys. A **22**, 511 (1989); R.R.P. Singh, M.E. Fisher, and R. Shankar, Phys. Rev. B **39**, 2562 (1989).

[5] E.H. Lieb and F.Y. Wu, Phys. Rev. Lett. **20**, 1445 (1968).

[6] J. E. Hirsch *et al.*, Phys. Rev. B **26**, 5033 (1982).

[7] H.J. Schulz, Phys. Rev. Lett. **64**, 2831 (1990); Int. J. Mod. Phys. B **5**, 57 (1991).

[8] J.E. Hirsch and D.J. Scalapino, Phys. Rev. B **27**, 7169 (1983); **29**, 5554 (1984).

[9] A.W. Sandvik, D.J. Scalapino, and C. Singh, Phys. Rev. B **48**, 2112 (1993).

[10] S.T. Chui and J.W. Bray, Phys. Rev. B **16**, 1329 (1977); W. Apel and T.M. Rice, *ibid.* **26**, 7063 (1982).

[11] Y. Suzumura and H. Fukuyama, J. Phys. Soc. Jpn. **53**, 3918 (1984).

[12] T. Giamarchi and H.J. Schulz, Phys. Rev. B **37**, 325 (1988).

[13] E. Abrahams *et al.*, Phys. Rev. Lett. **42**, 673 (1979).

[14] S.K. Ma, C. Dasgupta, and C.K. Hu, Phys. Rev. Lett. **43**, 1434 (1979); Phys. Rev. B **22**, 1305 (1980).

[15] Z.G. Soos and S.R. Bondeson, Solid State Commun. **35**, 11 (1980); S.R. Bondeson and Z.G. Soos, Phys. Rev. B **22**, 1793 (1980).

[16] J.E. Hirsch and J.V. José, J. Phys. C **13**, L53 (1980); Phys. Rev. B **22**, 5339 (1980).

[17] J.E. Hirsch, Phys. Rev. B **22**, 5355 (1980).

[18] J.E. Hirsch and R. Kariotis, Phys. Rev. B **32**, 7320 (1985); H.B. Schüttler, D.J. Scalapino, and P.M. Grant, *ibid.* **35**, 3461 (1987).

[19] A. Muramatsu and W. Hanke, Phys. Scr. **T13**, 319 (1986).

[20] A.W. Sandvik and D.J. Scalapino, Phys. Rev. B **47**, 10 090 (1993).

[21] Hathi-2, an array of 100 IMS T800 Transputers, at the Department of Computer Science, Åbo Akademi, Finland.

[22] A.W. Sandvik and J. Kurkijärvi, Phys. Rev. B **43**, 5950 (1991).

[23] A.W. Sandvik, J. Phys. A **25**, 3667 (1992).

[24] A.W. Sandvik (unpublished).

[25] D.C. Handscomb, Proc. Cambridge Philos. Soc. **58**, 594 (1962); **60**, 115 (1964).

[26] M. Ma, Phys. Rev. B **26**, 5097 (1982).